Supporting Information

Boosting Magnetoresistance in Manganese Phosphide Helimagnets through Iron Oxide Interface Strain Engineering

Nivarthana W.Y.A.Y. Mudiyanselage *[, a], Derick DeTellem [a], Yasinthara M. Wadumesthri [a], Amit Chanda [b], Anh Tuan Duong [c], Emmanuel Olawale [a], Humberto Rodriguez Gutierrez [a], Xiaomei Jiang [a], Sarath Witanachchi [a], and Manh-Huong Phan *[,a,d]

[a] Department of Physics, University of South Florida, Tampa, Florida 33620, USA

[b] Department of Energy Conversion and Storage, Technical University of Denmark, 2800 Kgs. Lyngby, Denmark

[c] Faculty of Materials Science and Engineering, Phenikaa University, Hanoi 12116, Vietnam

[d] Center for Materials Innovation and Technology, VinUniversity, Hanoi 100000, Vietnam

*Corresponding authors: nivarthanawa@usf.edu; phanm@usf.edu

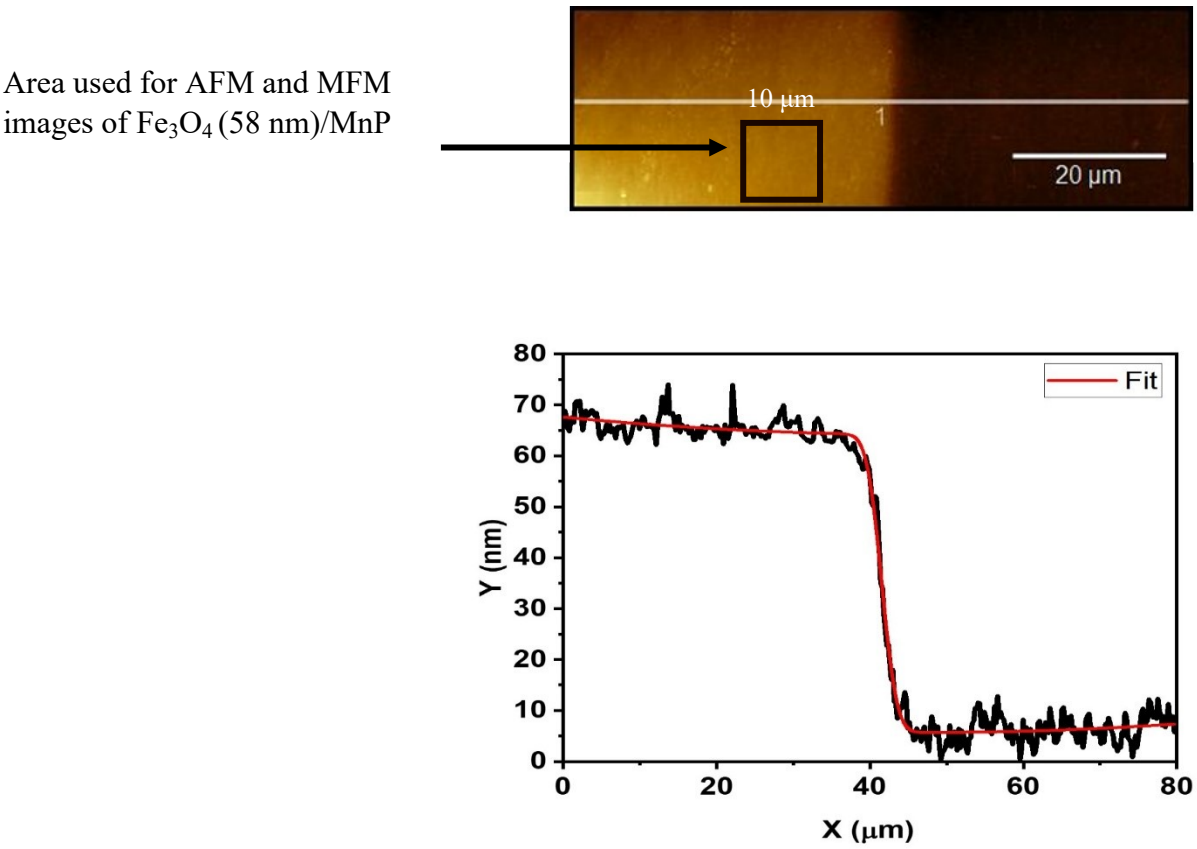

Figure S1. Step height profile (film thickness) measured with AFM. The fit (red line) was performed using Gwydion software and smooth bent step function. The resultant height, which corresponds to the thickness of Fe_3O_4 on MnP, is $58.491 \pm 0.56\ nm$.

(a)

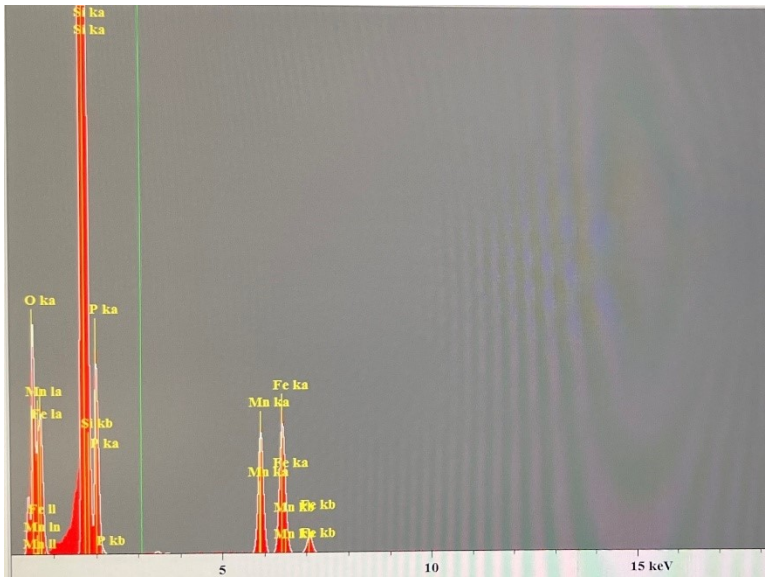

(b)

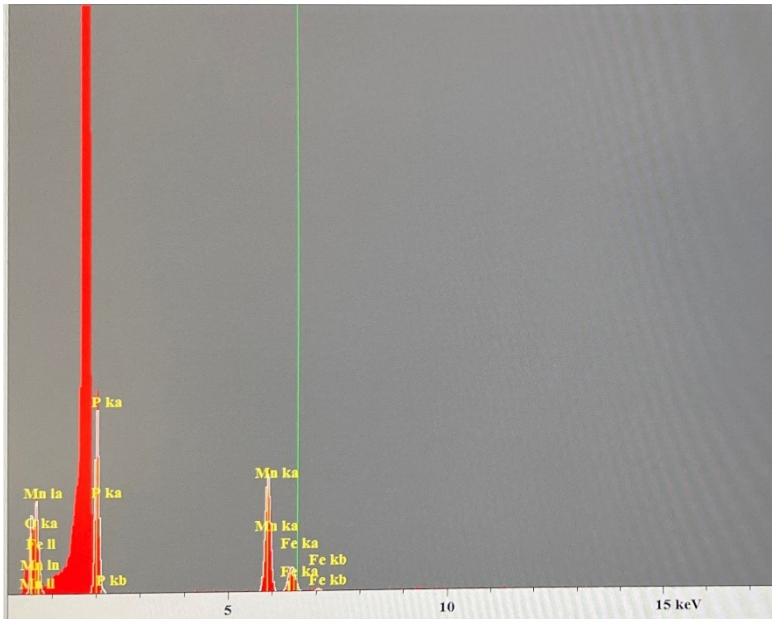

Figure S2. Energy dispersive spectroscopy (EDS) of (a) Fe_3O_4(58

nm)/MnP/Si and (b) Fe_3O_4(7 nm)/MnP/Si.

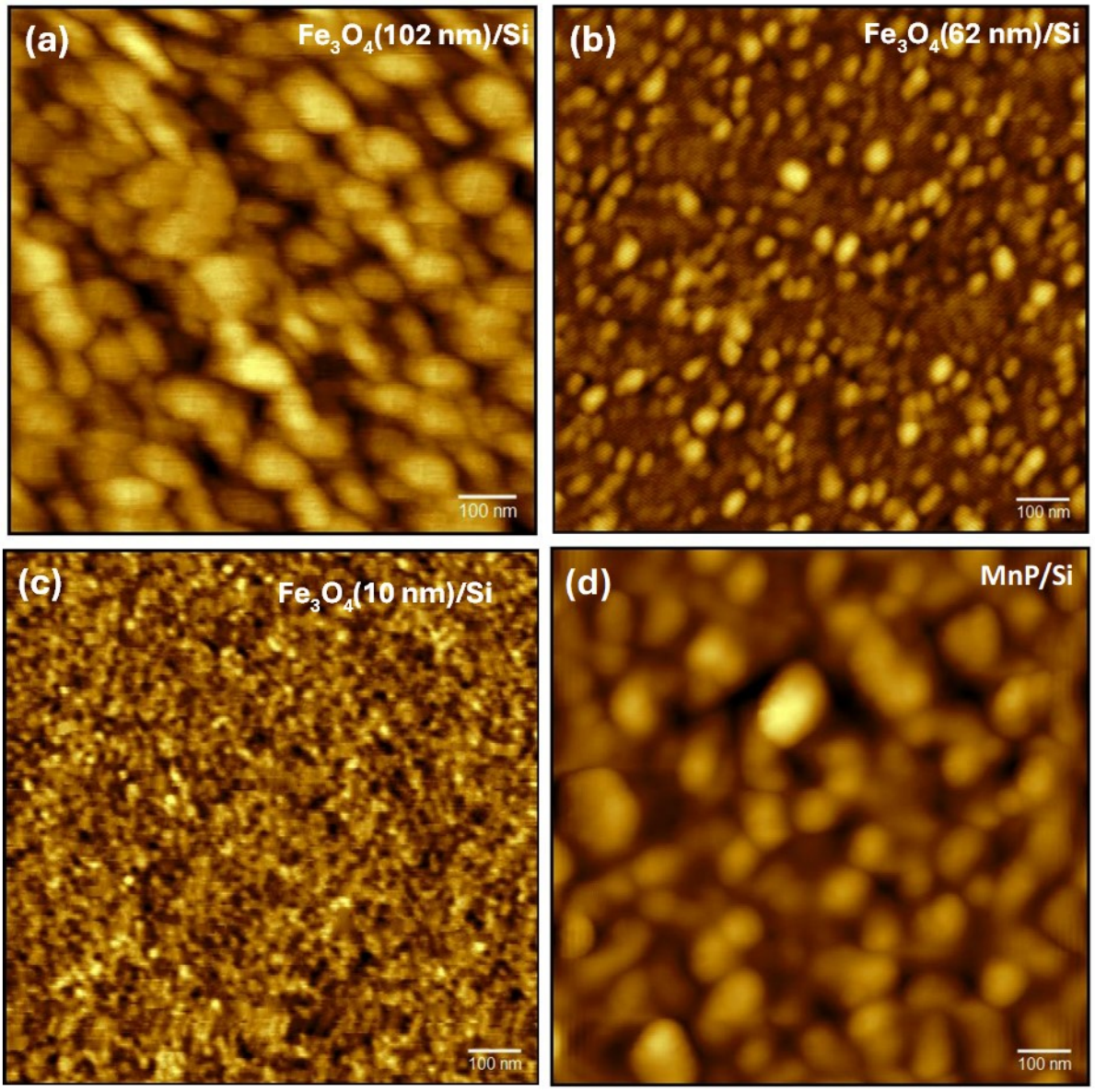

Figure S3. Atomic force microscopy (AFM) topography images of (a) Fe_3O_4(102 nm)/Si, (b) Fe_3O_4(62 nm)/Si, (c) Fe_3O_4(10 nm)/Si, and (d) MnP/Si.

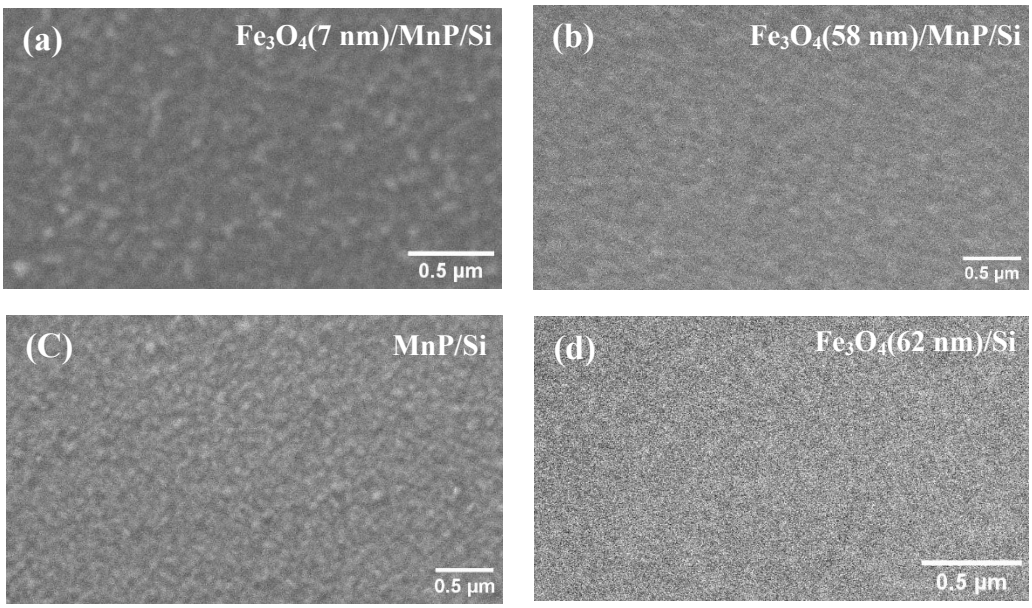

Figure S4. Scanning electron microscopy (SEM) images of (a) Fe_3O_4(7 nm)/MnP/Si, (b) Fe_3O_4(58 nm)/MnP/Si, (c) MnP/Si, and (d) Fe_3O_4(62 nm)/Si films.

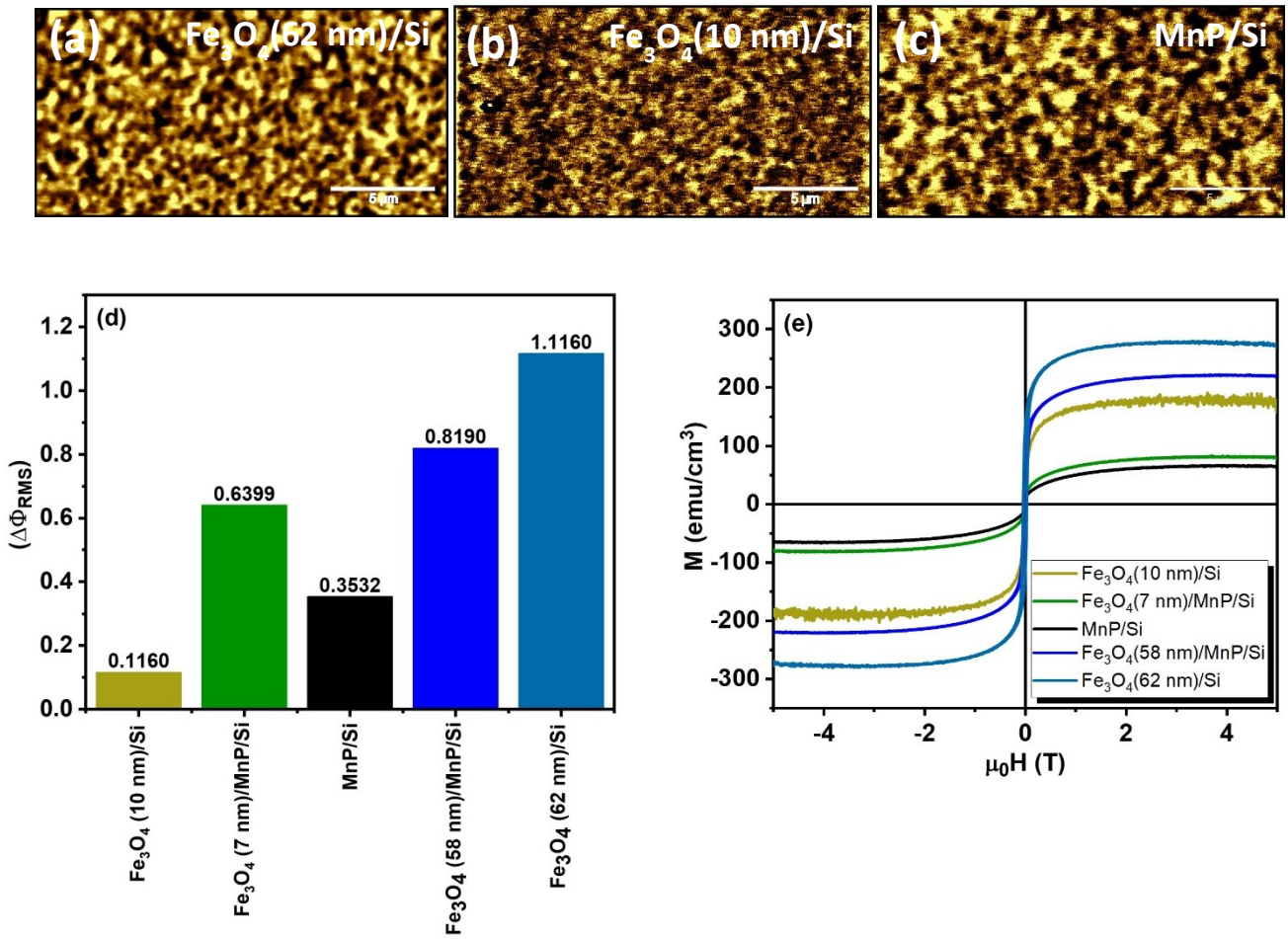

Figure S5. Magnetic force microscopy (MFM) images of (a) Fe_3O_4(62 nm)/Si, (b) Fe_3O_4(10 nm)/Si, (c) MnP/Si thin films, (d) the phase shift of RMS roughness ($^{\Delta\phi_{RMS}}$) and (e) in-plane magnetic field-dependent magnetization (M-H) curves for Fe_3O_4(10 nm)/Si, Fe_3O_4(7 nm)/MnP/Si, MnP/Si, Fe_3O_4(58 nm)/MnP/Si, and Fe_3O_4(62 nm)/Si at 300 K.

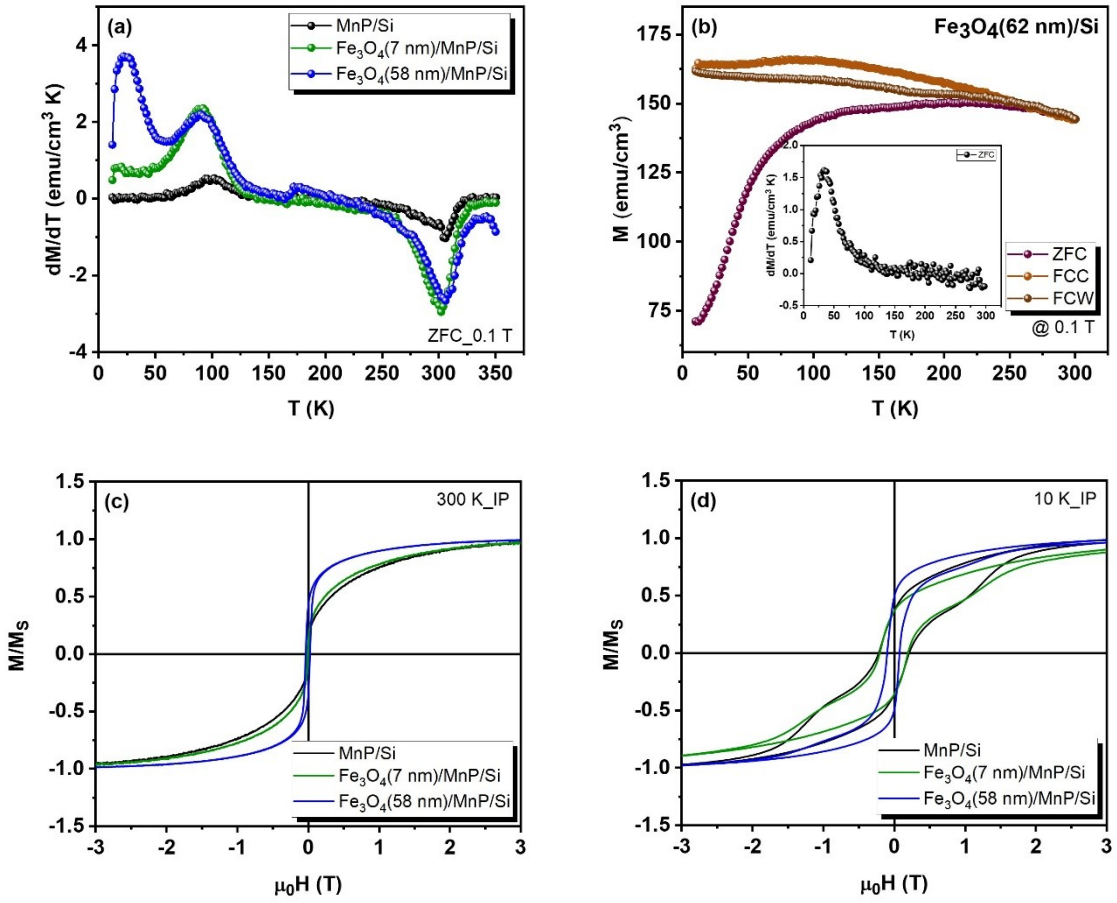

Figure S6. (a) First derivative of the temperature-dependent magnetization (d*M*/d*T*) under ZFC protocol at a magnetic field of 0.1 T for MnP/Si, Fe_3O_4(7 nm)/MnP/Si, and Fe_3O_4 (58 nm)/MnP/Si; (b) Temperature-dependent magnetization under ZFC, FCC, and FCC protocols for Fe_3O_4(62 nm)/Si under a magnetic field of 0.1 T. The inset indicates the first derivative of the temperature-dependent magnetization (d*M*/d*T*) under ZFC protocol with a magnetic field of 0.1 T; Magnetic field-dependent magnetization (normalized) for MnP/Si, Fe_3O_4(7 nm)/MnP/Si, and Fe_3O_4(58 nm)/MnP/Si at (c) 300 K, (d) 10 K for the in-plane configuration.

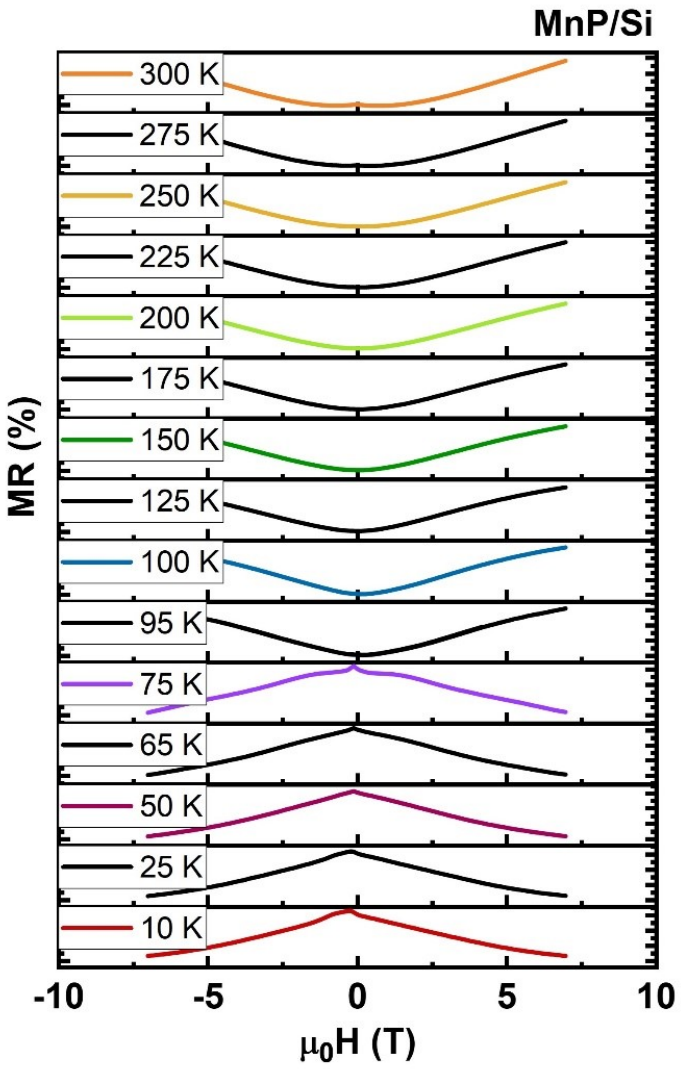

Figure S7. In-plane (IP) magnetic field-dependent magnetoresistance (MR) for the MnP/Si film.

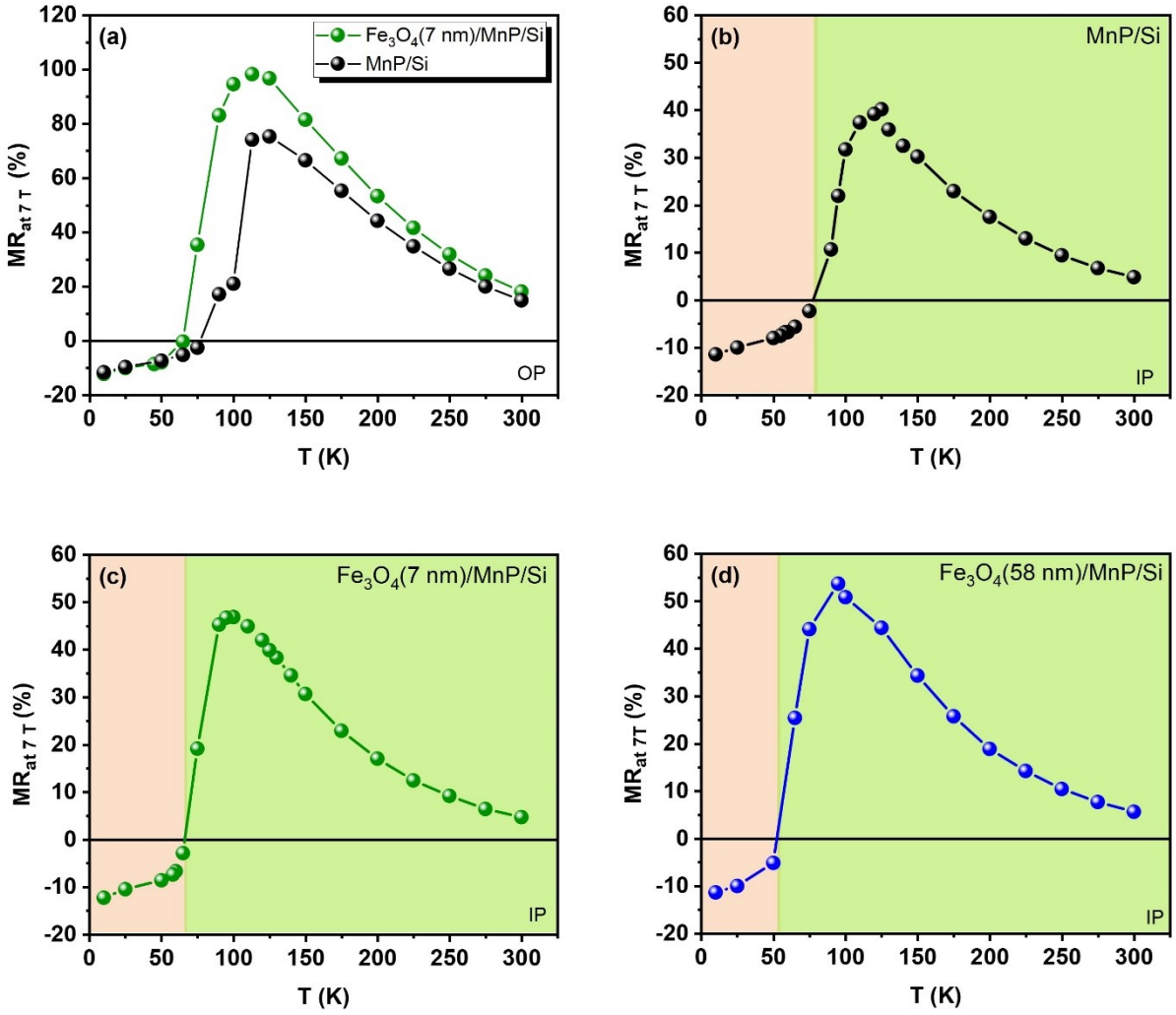

Figure S8. (a) Temperature-dependent out-of-plane (OP) magnetoresistance (MR) at 7 T for MnP/Si and Fe_3O_4(7 nm)/MnP/Si; Temperature-dependent in-plane (IP) magnetoresistance (MR) ratio at 7 T for (b) MnP/Si, (c) Fe_3O_4(7 nm)/MnP/Si, and (d) Fe_3O_4(58 nm)/MnP/Si.

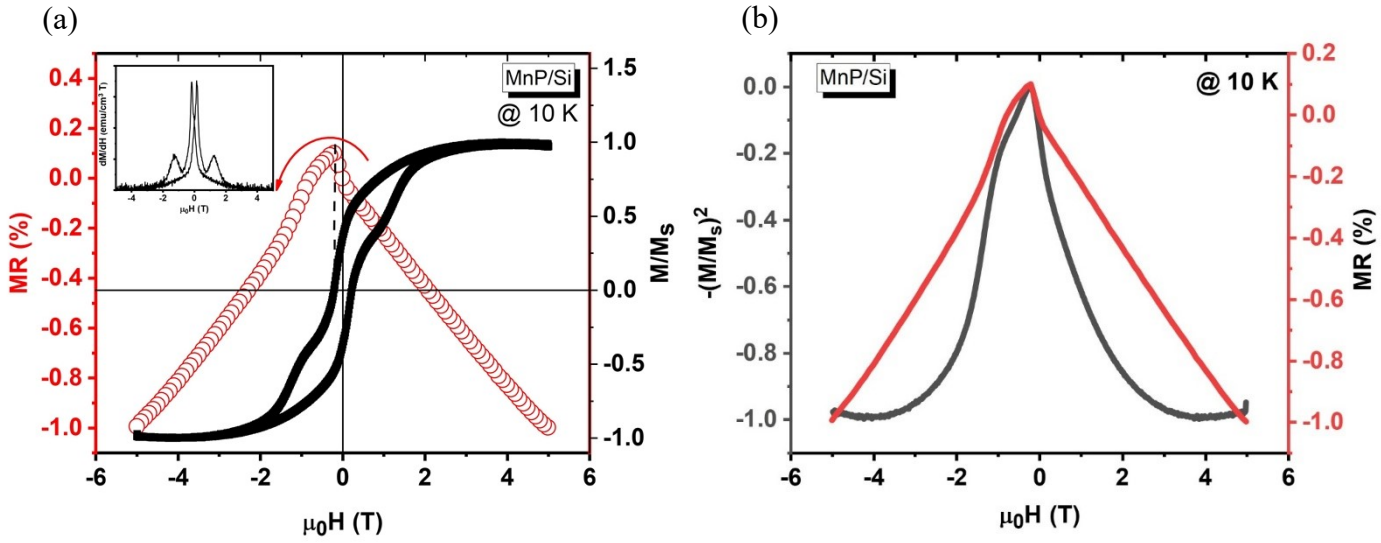

Figure S9. (a) Magnetic field-dependent magnetoresistance (MR, red curve) (from +7 T - -7 T) and magnetic field- dependent normalized magnetization (M/M_s) (black curve) measured at 10 K for MnP/Si, (b) The magnetic field-dependent magnetoresistance (MR, red curve) and normalized squared magnetization $-(M/M_s)^2$ (black curve) as a function of magnetic field at 10 K for MnP/Si. The inset of (a) indicates the magnetic field-dependent first derivative of magnetization (dM/dH) measured at 10 K for MnP/Si. The magnetic field is applied on a plane parallel to the plane of the film (in-plane).

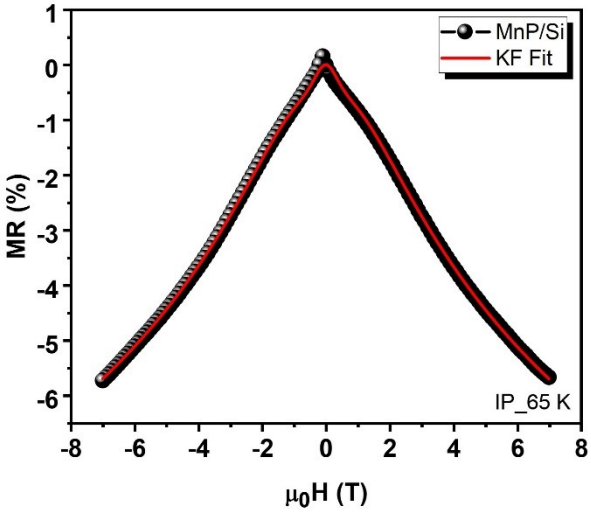

Figure S10. Magnetic field (in plane)-dependent longitudinal magnetoresistance at 65 K for the MnP/Si film. The solid (red) line represents the fitting curves using the KF model.

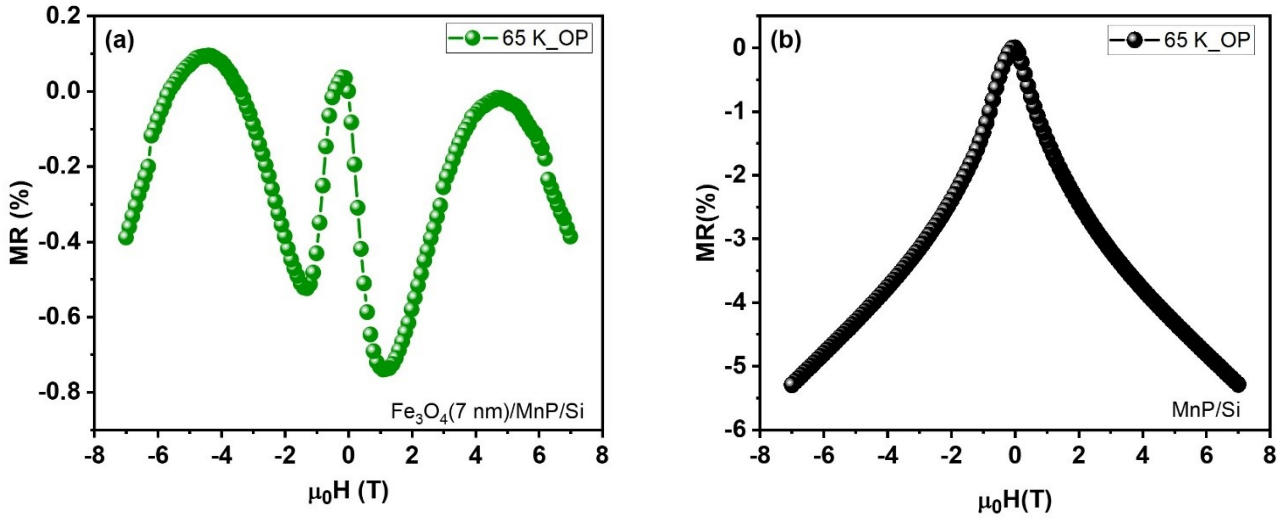

Figure S11. Magnetic field (out-of-plane (OP))-dependent magnetoresistance (MR) at 65 K for (a) Fe_3O_4(7 nm)/MnP/Si and (b) MnP/Si.

Table S1. Néel (T_N) and Curie (T_C) temperatures of the MnP/Si and Fe_3O_4/MnP/Si samples obtained from the first derivative of the temperature-dependent magnetization (dM/dT).

Sample	$T_N\,(K)$	$T_C\,(K)$
MnP/Si	102	306
Fe_3O_4(7 nm)/MnP/Si	91	304
Fe_3O_4 (58 nm)/MnP/Si	90	302

Table S2. The fitting parameters obtained using Equation (2) for MnP/Si and Fe_3O_4(7 nm)/MnP/Si.

MnP/Si				
T (K)	a	$b(T^{-1})$	$c(T^{-1})$	$d(T^{-1})$
50	1.6519 ± 0.0082	1.6658 ± 0.0842	2.0843 ± 0.1125	0.8956 ± 0.0349
58	1.5667 ± 0.0077	1.6700 ± 0.0748	1.9688 ± 0.0914	0.8727 ± 0.0303
60	1.5269 ± 0.0062	1.7877 ± 0.0700	2.0852 ± 0.0809	0.9223 ± 0.0266
65	1.4333 ± 0.0052	1.7972 ± 0.0558	1.9807 ± 0.0576	0.9012 ± 0.0201
Fe_3O_4(7 nm)/MnP/Si				
T (K)	a	$b(T^{-1})$	$c(T^{-1})$	$d(T^{-1})$
50	1.7122 ± 0.0134	1.4265 ± 0.1249	1.8305 ± 0.1919	0.8244 ± 0.0591
58	1.5097 ± 0.0097	1.7656 ± 0.1504	1.9928 ± 0.1974	0.9875 ± 0.0658
60	1.3973 ± 0.0087	1.9188 ± 0.1768	1.9870 ± 0.2165	1.0708 ± 0.0771
65	N/A	N/A	N/A	N/A